P{w[+m]FRT}42B P{PiM}46F P{PiM}47F. Clones of *tkv*, *sax*, *or shn* mutant cells were generated by flp-mediated recombination (flp is a yeast site-specific recombinase) [T. Xu and G. M. Rubin, *Development* **117**, 1223 (1993)]. Discs were stained with a Myc-specific monoclonal antibody, a rabbit antibody to cyclin B, or a rabbit antibody to ATONAL [S. S. Blair, *ibid.* **115**, 21 (1992); J. A. Williams, J. B. Bell, S. B. Carroll, *Genes Dev.* **5**, 2481 (1991)] with the use of a fluorescein conjugate to visualize the antibody to Myc and a Cy-5 conjugate for the antibody to cyclin B or ATONAL. Discs were labeled with propidium iodide after antibody staining [W.G. Whitfield, C. Gonzalez, G. Maldonado-Codina, D. M. Glover, *EMBO J.* **9**, 2563 (1990)]. Thirteen out of 14 tkv^5 clones that encompassed the anterior half of the MF, and 2 out of 7 clones in the posterior half, had ectopic cyclin B expression. Nineteen of 29 *shnIB* clones and 10 of 16 sax^4 clones had aberrant cyclin B expression in the MF. Cyclin B misexpression was less severe in *shnIB* and sax^4 clones, particularly if they were near the equator. Six tkv^5 clones in the MF were examined for their effect on *atonal* expression.

19. Clones of *tkv* in adult eyes were induced as above except that males of the genotype *w*, tkv^5 *P{ry[+]hsp70:neo FRT}40A/In(2LR)Gla* were crossed to females of the genotype *y w P{ry[+]hsp70-flp}, P{w[+]}30C P{ry[+] hsp70:neoFRT}40A*. Sections of adult eyes were made as described [N. L. Brown, C. A. Sattler, D. R. Markey, S. B. Carroll, *Development* **113**, 1245 (1991)]. Ten clones were scored from six sectioned eyes. Seventy-one ommatidia with some or all retinal cells mutant for *tkv* had a normal configuration of seven retinal cells. Thirteen mutant ommatidia were defective. The defective ommatidia contained from four to six retinal cells. The identify of the missing cell varied, although the altered shape of the clusters did not always permit the identify of the missing cell or cells to be established.

20. We thank N. Perrimon, V. Twombly, M. Singer, and W. M. Gelbert for fly stocks; S. Blair, Y. Jan, W. Whitfield, and D. Glover for antibodies; the W. M. Keck Foundation Neural Imaging Lab for use of their confocal microscope; J. Hudzinski, A. Kusano, and C. A. Sattler for technical help; and S. B. Carroll, K. Basler, and U. Heberlein for comments on the manuscript. Supported by grants from the NIH National Center for Research Resources to F.M.H. and from the National Cancer Institute. S.B.S. is a fellow of the Alfred P. Sloane Foundation.

22 August 1996; accepted 29 October 1996

Activation of Interferon-γ Inducing Factor Mediated by Interleukin-1β Converting Enzyme

Yong Gu, Keisuke Kuida, Hiroko Tsutsui, George Ku, Kathy Hsiao, Mark A. Fleming, Nobuki Hayashi, Kazuya Higashino, Haruki Okamura, Kenji Nakanishi, Masashi Kurimoto, Tadao Tanimoto, Richard A. Flavell, Vicki Sato, Matthew W. Harding, David J. Livingston, Michael S.-S. Su*

The interleukin-1β (IL-1β) converting enzyme (ICE) processes the inactive IL-1β precursor to the proinflammatory cytokine. ICE was also shown to cleave the precursor of interferon-γ inducing factor (IGIF) at the authentic processing site with high efficiency, thereby activating IGIF and facilitating its export. Lipopolysaccharide-activated ICE-deficient ($ICE^{-/-}$) Kupffer cells synthesized the IGIF precursor but failed to process it into the active form. Interferon-γ and IGIF were diminished in the sera of $ICE^{-/-}$ mice exposed to *Propionibacterium acnes* and lipopolysaccharide. The lack of multiple proinflammatory cytokines in $ICE^{-/-}$ mice may account for their protection from septic shock.

ICE is a member of the growing family of ICE-like cysteine proteases (caspases) with a substrate specificity for aspartate (*1*). ICE (caspase-1) was identified on the basis of its proteolytic activity for cleaving the inactive IL-1β precursor into the 17-kD mature cytokine (*2*). ICE-deficient mice are impaired in their production of mature IL-1β (*3*), which establishes the physiological role of ICE in the processing and export of IL-1β. In contrast to IL-1β–deficient mice (*4*), $ICE^{-/-}$ mice also have less IL-1α, tumor necrosis factor–α (TNF-α), and IL-6 and are resistant to septic shock induced by endotoxin (*3*), which suggests that ICE may have additional functions in the regulation of the immune system.

Y. Gu, G. Ku, K. Hsiao, M. A. Fleming, V. Sato, M. W. Harding, D. J. Livingston, M. S.-S. Su, Vertex Pharmaceuticals Inc., 130 Waverly Street, Cambridge, MA 02139, USA.
K. Kuida, Tokyo Metropolitan Institute of Medical Science, Tokyo, Japan.
H. Tsutsui, N. Hayashi, K. Higashino, H. Okamura, K. Nakanishi, Hyogo College of Medicine, 1-1, Mukogawa-cho, Nishinomiya, Japan.
M. Kurimoto and T. Tanimoto, Fujisaki Institute, Hayashibara Biochemical Laboratories, Hayashibara Company Inc., Okayama, Japan.
R. A. Flavell, Howard Hughes Medical Institute, Yale University School of Medicine, New Haven, CT 06510, USA.

IGIF, an ~18-kD polypeptide that stimulates production of interferon-γ (IFN-γ) by T cells (*5*), is synthesized as a polypeptide precursor (proIGIF) devoid of a conventional signal sequence (*6*). The precursor of IGIF is cleaved after Asp^{35} (*6*), which suggests that an aspartate-specific protease may be involved. Two families of proteases with substrate specificity for aspartate have been identified; these include the ICE family of cysteine proteases and granzyme B, a serine protease involved in cytotoxic lymphocyte–mediated cell killing and activation of ICE-like cysteine proteases (*7*, *8*). Therefore, we investigated whether one or more of the ICE-family proteases or granzyme B may be involved in the processing of proIGIF and investigated the role that such a cleavage may have in the function of IGIF.

We first used transient coexpression in COS cells (*9*) to determine whether proIGIF could be processed by some of the known ICE-family proteases (Fig. 1A). Coexpression of proIGIF with ICE or its homolog TX (caspase-4) (*10*) resulted in the cleavage of proIGIF into a polypeptide similar in size to the naturally occurring 18-kD IGIF. Single point mutations of the catalytic cysteine residues that inactivate ICE and TX (*11*) blocked cleavage. Coexpression with CPP32 (caspase-3), a protease involved in programmed cell death (apoptosis) (*12*), resulted in the cleavage of proIGIF into a ~14-kD polypeptide, whereas CMH-1 (caspase-7), a homolog of CPP32 (*13*), did not appreciably cleave proIGIF. Thus, ICE and TX could cleave proIGIF into a polypeptide similar to the naturally occurring IGIF.

We examined the cleavage of proIGIF by these proteases in vitro with the use of purified recombinant $(His)_6$-tagged proIGIF as a substrate (*14*). ICE cleaved the 24-kD proIGIF into two polypeptides of ~18 and ~6 kD (Fig. 1B). The 18-kD polypeptide comigrated with recombinant mature IGIF upon SDS–polyacrylamide gel electrophoresis (PAGE) and contained the same amino acid residues (Asn-Phe-Gly-Arg-Leu) at its NH_2-terminus as did the naturally occurring murine IGIF, indicating that ICE cleaved proIGIF at the authentic processing site (Asp^{35}-Asn^{36}) (*6*). This cleavage was specific with a catalytic efficiency (k_{cat}/K_m, where K_m is the Michaelis constant) of 1.4×10^7 M^{-1} s^{-1} ($K_m = 0.6 \pm 0.1$ μM; $k_{cat} = 8.6 \pm 0.3$ s^{-1}) (*15*) and was inhibited by the specific ICE inhibitors Ac-Tyr-Val-Ala-Asp-aldehyde (*2*) and Cbz-Val-Ala-Asp-[(2,6-dichlorobenzoyl)oxy]methyl ketone (*16*). Recombinant $(His)_6$-tagged human proIGIF was also cleaved by ICE with a similar specificity. Although proIGIF had no detectable IFN-γ–inducing activity, ICE-cleaved proIGIF was active in inducing IFN-γ production in T helper type 1 (T_H1) cells (Fig. 1C) (*17*). TX also cleaved proIGIF into polypeptides of similar size; however, its catalytic efficiency was about two orders of magnitude lower than that of ICE. In a manner consistent with the observation from the COS cell experiments, CPP32 cleaved proIGIF at a different site (Asp^{69}-Ile^{70}) and the resulting polypeptides had little IFN-γ–inducing activity, whereas CMH-1 and granzyme B did not cleave proIGIF. Thus, both in COS cells and in vitro, ICE can process the inactive IGIF precursor at the authentic maturation site to generate the biologically active form of IGIF.

IGIF is produced by activated Kupffer cells and macrophages in vivo and is exported from the cells upon stimulation by endotoxin (*5*, *6*). We used the COS cell coexpression system to investigate whether the cleavage of proIGIF by ICE would facilitate the export of mature IGIF, as in the case of IL-1β (*2*). COS cells coexpressing proIGIF and ICE were labeled with [^{35}S]methionine (*18*). COS cell lysates and conditioned medium were immunoprecipitated with an antiserum to IGIF that recognizes both the precursor and the mature form (*6*) (Fig. 2A). An 18-kD polypeptide corresponding to the mature IGIF was detected in the conditioned medium of COS cells coexpressing proIGIF and ICE, whereas COS cells expressing proIGIF alone or with the inactive ICE mutant exported only a very small amount of proIGIF. We estimated by PhosphorImager analysis that ~10% of the mature IGIF was exported from transfected cells, whereas <1% of proIGIF was exported. We also measured the presence of IFN-γ–inducing activity in cell lysates and in the conditioned media of transfected cells (*19*). IFN-γ–inducing activity was detected in both cell lysates and conditioned medium of COS cells coexpressing proIGIF and ICE, but not those of cells expressing proIGIF or ICE alone (Fig. 2B). The relative amounts of mature IGIF in the medium and in cell lysates (*19*) indicated that the secreted IGIF was at least as active as the cytosolic mature IGIF. Thus, ICE cleavage of proIGIF can facilitate the export of mature and active IGIF from cells.

To study the role of ICE in the activation and export of IGIF under physiological conditions, we examined the processing and export of IGIF from lipopolysaccharide (LPS)-stimulated Kupffer cells isolated from *Propionibacterium acnes*–elicited wild-type and ICE$^{-/-}$ mice (*20*). Although lysates of Kupffer cells from wild-type and ICE$^{-/-}$ mice contained similar amounts of IGIF [as determined by an enzyme-linked immunosorbent assay (ELISA) that recognized both proIGIF and mature IGIF], IGIF was detected in the conditioned medium of wild-type cells but not in that of ICE$^{-/-}$ cells (Fig. 3A). Metabolic labeling and immunoprecipitation experiments confirmed the presence of unprocessed proIGIF in both wild-type and ICE$^{-/-}$ Kupffer cell lysates. However, the 18-kD mature IGIF was present only in the conditioned medium of wild-type Kupffer cell cultures and not in that of ICE$^{-/-}$ cultures (Fig. 3B). Similarly, the conditioned medium of LPS-stimulated wild-type adherent splenocytes contained IFN-γ–inducing activity that was sensitive to a neutralizing antibody to IGIF (anti-IGIF); this activity was re-

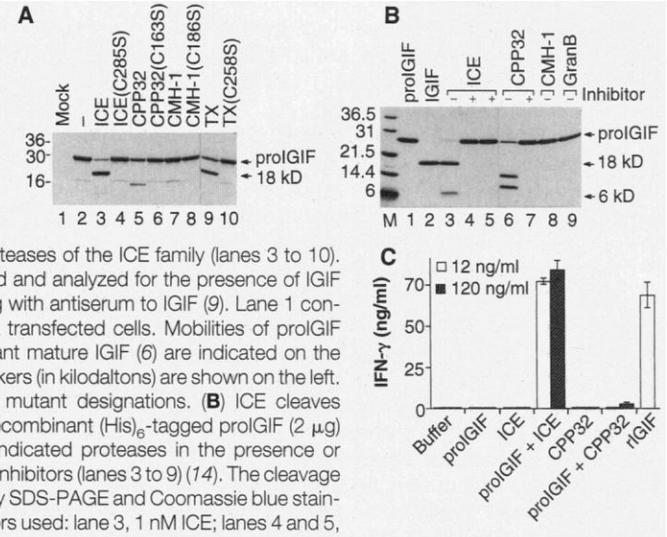

Fig. 1. ICE cleaves and activates proIGIF. (**A**) ICE cleaves proIGIF in COS cells. COS cells were transfected with an expression plasmid for proIGIF alone (lane 2) or in combination with the indicated expression plasmids encoding wild-type or inactive mutants of proteases of the ICE family (lanes 3 to 10). Cell lysates were prepared and analyzed for the presence of IGIF protein by immunoblotting with antiserum to IGIF (*9*). Lane 1 contained lysates from mock transfected cells. Mobilities of proIGIF and the 18-kD recombinant mature IGIF (*6*) are indicated on the right; molecular mass markers (in kilodaltons) are shown on the left. C, cysteine; S, serine in mutant designations. (**B**) ICE cleaves proIGIF in vitro. Purified recombinant $(His)_6$-tagged proIGIF (2 μg) was incubated with the indicated proteases in the presence or absence of ICE or CPP32 inhibitors (lanes 3 to 9) (*14*). The cleavage products were analyzed by SDS-PAGE and Coomassie blue staining. Proteases and inhibitors used: lane 3, 1 nM ICE; lanes 4 and 5, 1 nM ICE with 10 nM Cbz-Val-Ala-Asp-[(2,6-dichlorobenzoyl)oxy]methyl ketone and 100 nM Ac-Tyr-Val-Ala-Asp-aldehyde, respectively; lanes 6 and 7, 15 nM CPP32 with and without 400 nM Ac-Asp-Glu-Val-Asp-aldehyde (*12*), respectively; lane 8, 100 nM CMH-1; lane 9, granzyme B (10 U/ml). Lanes 1 and 2 contained proIGIF and recombinant mature IGIF (*6*), respectively; lane M, molecular mass markers. NH_2-terminal amino acid sequencing indicated that ICE cleaved proIGIF at the authentic processing site Asp^{35}-Asn^{36}, whereas CPP32 cleavage occurred at Asp^{69}-Ile^{70}. (**C**) ICE cleavage activates proIGIF. Uncleaved or ICE- or CPP32-cleaved products of proIGIF, or recombinant mature IGIF (rIGIF), were added to A. E7 cell cultures to a final concentration of 12 or 120 ng/ml; 18 hours later, IFN-γ in the culture medium was determined by ELISA (*17*). The data represent the average of three determinations.

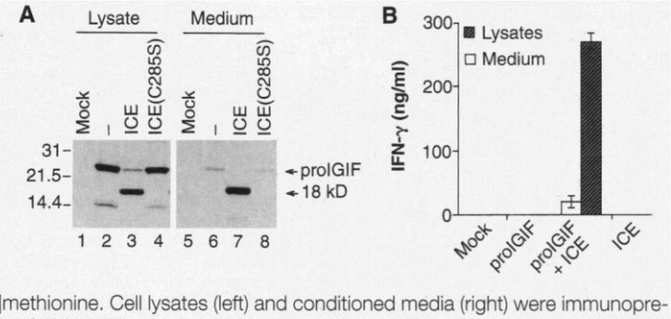

Fig. 2. Processing of proIGIF by ICE facilitates the export of IGIF. (**A**) COS cells transfected with an expression plasmid for proIGIF alone (lanes 2 and 6) or in combination with an expression plasmid encoding wild-type (lanes 3 and 7) or inactive mutant (lanes 4 and 8) ICE were metabolically labeled with [^{35}S]methionine. Cell lysates (left) and conditioned media (right) were immunoprecipitated with antiserum to IGIF (*18*). The immunoprecipitated proteins were analyzed by SDS-PAGE and fluorography. Fluorograms were exposed for 10 hours (left) and 3 days (right), respectively. Mobilities of proIGIF and the 18-kD mature IGIF are indicated on the right; molecular masses are shown on the left. Quantitative PhosphorImager analysis indicated that ~10% of mature IGIF is exported out of the cells, whereas only 1% of proIGIF is exported. (**B**) Cell lysates and conditioned medium from similarly transfected but unlabeled COS cells were assayed for IFN-γ–inducing activity (*19*) as in Fig. 1C.

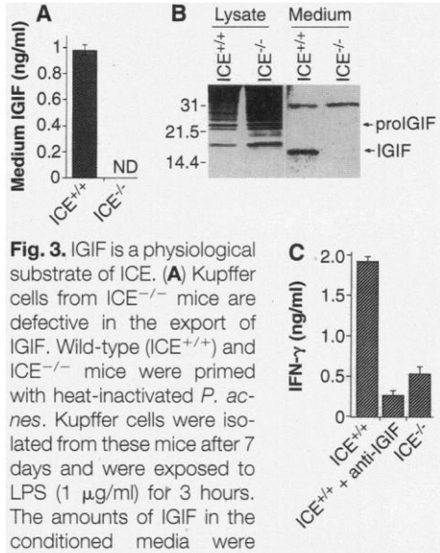

Fig. 3. IGIF is a physiological substrate of ICE. (**A**) Kupffer cells from ICE$^{-/-}$ mice are defective in the export of IGIF. Wild-type (ICE$^{+/+}$) and ICE$^{-/-}$ mice were primed with heat-inactivated *P. acnes*. Kupffer cells were isolated from these mice after 7 days and were exposed to LPS (1 μg/ml) for 3 hours. The amounts of IGIF in the conditioned media were measured by ELISA (*20*). ND, not detectable (<0.1 ng/ml). (**B**) Kupffer cells isolated from ICE$^{+/+}$ and ICE$^{-/-}$ mice as above were metabolically labeled with [^{35}S]methionine in the presence of LPS (1 μg/ml). Cell lysates and conditioned media were immunoprecipitated and analyzed by SDS-PAGE and fluorography. Mobilities of proIGIF and the 18-kD mature IGIF are indicated on the right; molecular mass markers are shown on the left. (**C**) ICE$^{-/-}$ splenocytes are deficient in IGIF production. Conditioned media from LPS-stimulated ICE$^{+/+}$ or ICE$^{-/-}$ adherent splenocytes were added to wild-type nonadherent splenic T cell cultures in the presence or absence of neutralizing anti-IGIF. IFN-γ concentrations in the medium were determined 20 hours later.

duced in the medium of adherent splenocytes of ICE$^{-/-}$ mice (Fig. 3C). The absence of IGIF in the conditioned medium of ICE$^{-/-}$ Kupffer cells and adherent splenocytes established that the processing of proIGIF by ICE is required for the export of IGIF.

The sera of ICE$^{-/-}$ mice stimulated by *P. acnes* and LPS (*21*) also contained reduced amounts of IGIF (Fig. 4A). This finding may account for the lower concentrations of IFN-γ in the sera of treated ICE$^{-/-}$ mice (Fig. 4B) (*22*) because we observed no difference between wild-type and ICE$^{-/-}$ mice in the production of IL-12, the other cytokine known to induce IFN-γ (*23*). Nonadherent splenocytes from wild-type and ICE$^{-/-}$ mice produced similar amounts of IFN-γ when stimulated with IGIF in vitro. Administration of recombinant mature IGIF (*6*) into ICE$^{-/-}$ mice restored IFN-γ production in these animals (Fig. 4B), which indicated that the impaired production of IFN-γ was not the result of a defect in the T cells of ICE$^{-/-}$ mice. Moreover, injection of neutralizing anti-IGIF suppressed IFN-γ production in wild-type animals stimulated by *P. acnes* and LPS (Fig. 4C). The defect in IFN-γ production in ICE$^{-/-}$ mice was comparable in magnitude to the defect in IL-1β release, whereas only slight reductions were observed for TNF-α or IL-6 (*3*). Thus, ICE is necessary for processing of the IGIF precursor and export of active IGIF.

IFN-γ and IL-1β are pleiotropic cytokines that contribute to the pathology associated with a variety of infectious, inflammatory, and autoimmune diseases. IFN-γ promotes the activation of macrophages and natural killer cells and contributes to the regulation of T helper cell immune responses, whereas IL-1β stimulates proinflammatory responses in neutrophils, endothelial cells, synovial cells, osteoclasts, and other cell types (*24*). The processing of proIGIF by ICE establishes a link in the regulation of IL-1β and IFN-γ production with implications for monocyte- or macrophage-mediated and T cell–mediated immune functions. IFN-γ can increase the expression of ICE in monocytic cells (*25*), which suggests a positive-feedback regulation between ICE and IFN-γ that may further enhance the production of IGIF and IL-1β. However, IFN-γ production by antigen-specific T cells may not be dependent on the ICE-IGIF pathway, because mitogen (concanavalin A) or antigen stimulation of splenic T cells from ICE$^{-/-}$ mice elicited release of normal amounts of IFN-γ (*26*). T cell proliferation and delayed-type hypersensitivity responses are normal in ICE$^{-/-}$ mice after a secondary exposure to *Listeria monocytogenes* (*22*). Thus, the ICE-IGIF pathway of IFN-γ production may be more relevant in vivo to monocyte- or macrophage-mediated inflammatory insults, as opposed to T cell–dependent immune responses.

ICE processing of proIGIF and IFN-γ production may be central events in the pathogenesis of sepsis. Mice lacking IFN-γ or its receptor are resistant to endotoxic shock (*27*), and neutralizing anti-IGIF prevents LPS-induced hepatic injury in *P. acnes*–primed mice (*6*). These observations suggest that the reduced concentrations of IL-1β, IGIF, and IFN-γ in LPS-exposed ICE$^{-/-}$ mice (*3*, *22*) account for their increased resistance to LPS-induced sepsis relative to mice lacking a functional IL-1β gene (*4*), which have a normal septic response. The involvement of ICE in the regulation of these multiple proinflammatory cytokines should be considered in future evaluations of the therapeutic effects of ICE inhibition.

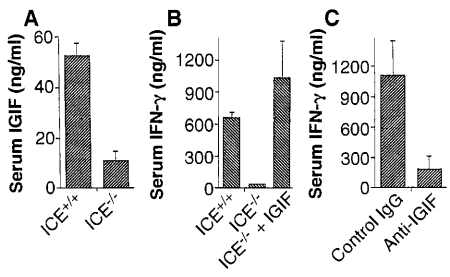

Fig. 4. ICE-deficient mice have reduced serum concentrations of IGIF and IFN-γ. (**A** and **B**) Wild-type (ICE$^{+/+}$) and ICE$^{-/-}$ mice (n = 3) primed with heat-inactivated *P. acnes* were exposed to LPS or LPS plus recombinant IGIF (*21*), and the concentrations of IGIF (A) and IFN-γ (B) in the sera were measured by ELISA 3 hours after LPS exposure. (**C**) Anti-IGIF blocks IFN-γ production in wild-type animals. Wild-type mice (n = 3) primed with *P. acnes* were injected with LPS plus anti-IGIF. Serum concentrations of IFN-γ were determined 3 hours later. IgG, immunoglobulin G.

REFERENCES AND NOTES

1. E. S. Alnemri *et al.*, *Cell* **87**, 171 (1996).
2. D. P. Cerretti *et al.*, *Science* **256**, 97 (1992); N. A. Thornberry *et al.*, *Nature* **356**, 768 (1992).
3. K. Kuida *et al.*, *Science* **267**, 2000 (1995); P. Li *et al.*, *Cell* **80**, 401 (1995).
4. H. Zheng *et al.*, *Immunity* **3**, 9 (1995).
5. H. Okamura *et al.*, *Infect. Immun.* **63**, 3966 (1995).
6. H. Okamura *et al.*, *Nature* **378**, 88 (1995); S. Ushio *et al.*, *J. Immunol.* **156**, 4274 (1996).
7. J. W. Heusel, R. L. Wesselschmidt, S. Shresta, J. H. Russell, T. J. Ley, *Cell* **76**, 977 (1994); A. J. Darmon, D. W. Nicholson, R. C. Bleackley, *Nature* **377**, 446 (1995); L. T. Quan *et al.*, *Proc. Natl. Acad. Sci. U.S.A.* **93**, 1972 (1996).
8. Y. Gu *et al.*, *J. Biol. Chem.* **271**, 10816 (1996).
9. A 0.6-kb cDNA encoding full-length murine proIGIF (*6*) was ligated into the mammalian expression vector pCDLSRα (*28*). Plasmids for the expression of active human ICE (*11*), TX (*10*), and CMH-1 (*13*) lacking the prosequence were as described. Expression plasmid for the active form of CPP32 lacking the prosequence (*12*) was constructed similarly in the pCDLSRα vector. Plasmids (3 μg) were transfected into COS cells in 35-mm dishes by the DEAE-dextran method (*11*). Twenty-four hours later, cells were lysed and the lysates were subjected to SDS-PAGE and immunoblotting with an antiserum to IGIF (*6*).
10. C. Faucheu *et al.*, *EMBO J.* **14**, 1914 (1995).
11. Y. Gu *et al.*, *ibid.*, p. 1923.
12. T. Fernandes-Alnemri, G. Litwack, E. S. Alnemri, *J. Biol. Chem.* **269**, 30761 (1994); D. W. Nicholson *et al.*, *Nature* **376**, 37 (1995); M. Tewari *et al.*, *Cell* **81**, 801 (1995).
13. J. A. Lippke, Y. Gu, C. Sarnecki, P. R. Caron, M. S.-S. Su, *J. Biol. Chem.* **271**, 1825 (1996).
14. Expression plasmid for $(His)_6$-proIGIF was created by introducing Nde I sites at the ends of murine proIGIF cDNA coding sequence (*6*) and ligating into *Escherichia coli* expression vector pET-15B (Novagen). The *E. coli* strain BL21(DE3) carrying the plasmid was induced with isopropyl-1-thio-β-D-galactopyranoside. $(His)_6$-proIGIF protein was purified from soluble fractions by Ni–nitrilotriacetic acid–agarose (Qiagen) chromatography according to the manufacturer's instructions. In vitro cleavage reactions by ICE and ICE-like proteases were carried out as in (*29*). Conditions for cleavage by granzyme B were as in (*8*). Cleavage products were analyzed by SDS-PAGE on 16% gels and Coomassie blue staining and were subjected to NH_2-terminal amino acid sequencing with an ABI automated peptide sequencer.
15. [^{35}S]methionine-labeled proIGIF [~3000 cpm, prepared by in vitro transcription and translation with the TNT T7 coupled reticulocyte lysate system (Promega) and proIGIF cDNA in pSP73 vector as template] was incubated in reaction mixtures of 60 μl containing 0.1 to 1 nM recombinant ICE and 190 nM to 12 μM unlabeled proIGIF for 8 to 10 min at 37°C. Cleavage product concentrations were determined by SDS-PAGE and PhosphorImager analysis. The kinetic parameters were calculated by nonlinear regression fitting of the rate versus concentration data to the Michaelis-Menten equation by means of the program Enzfitter (Biosoft).
16. R. E. Dolle *et al.*, *J. Med. Chem.* **37**, 563 (1994).
17. The T_H1 A. E7 cells (*30*) (1.3×10^5 cells in 0.15 ml) or nonadherent splenic T cells (8×10^5 cells) in 96-well plates were treated with IGIF or conditioned medium for 18 to 20 hours, and the culture supernatants were assayed for IFN-γ by ELISA (Endogen, Cambridge, MA).
18. COS cells (3.5×10^5 cells in a 35-mm dish) were labeled for 7 hours with 1 ml of methionine-free Dulbecco's modified Eagle's medium (DMEM) containing 2.5% normal DMEM, 1% dialyzed fetal bovine serum (FBS), and [^{35}S]methionine (300 μCi/ml; [^{35}S]Express Protein Labeling Mix, New England Nuclear). Cell lysates [prepared in 20 mM Hepes (pH 7.2), 150 mM NaCl, 0.1% Triton X-100, 5 mM *N*-ethylmaleimide, 1 mM phenylmethylsulfonyl fluoride, and leupeptin (2.5 μg/ml)] or conditioned medium were immunoprecipitated with the antiserum to IGIF (*6*).
19. COS cells (3.5×10^5 cells in a 35-mm dish) were transfected and grown in 1 ml of medium for 18 hours. Medium was harvested and used at 1:10 final dilution in the IFN-γ induction assay (*17*); COS cell pellets from the same transfection were lysed in 100 μl of 20 mM Hepes (pH 7.0) by three cycles of freezing and thawing. Lysates were cleared by centrifugation and were used at 1:10 dilution in the assay. On the basis of our analysis that 10% mature IGIF was exported out of the cells, we estimated that the mature IGIF concentration in lysates is ~90 times that of the conditioned medium.
20. Wild-type or ICE-deficient mice were injected intraperitoneally with 1 mg of heat-killed *P. acnes* (*5*). Kupffer cells were prepared 7 days later (*31*), except that nycodenz gradient was used instead of metrizamide. For each experiment, Kupffer cells (1×10^6 cells per milliliter) from two or three animals were pooled and cultured in RPMI 1640 supplemented with 10% FBS and LPS (1 μg/ml; Difco, *E. coli* strain 055:B5). Cell lysates and conditioned media were prepared 3 hours later. IGIF was determined by ELISA with protein G–purified rabbit polyclonal antibody to murine IGIF (*6*). Metabolic labeling and immunoprecipitation experiments were carried out as for COS cells (*18*) except that methionine-free RPMI 1640 was used in place of DMEM. To prepare conditioned medium of LPS-stimulated adherent splenocytes, we cultured total splenic cells (6×10^7 cells in 1 ml) from wild-type or ICE$^{-/-}$ mice for 1 hour. Adherent cells were then stimulated with LPS (50 ng/ml) for 5 hours. Conditioned media were harvest-

ed and used at 1:4 dilution in the IFN-γ assay (*17*) in the presence or absence of anti-IGIF (25 μg/ml) (*6*).
21. Wild-type or ICE-deficient mice were primed with *P. acnes* (*20*). Seven days later, mice were exposed to LPS (1 μg, intravenously). In some experiments, recombinant mature IGIF (1 μg) or protein G–purified anti-IGIF (250 μg) was coinjected with LPS; sera were collected 3 hours after LPS exposure.
22. Reduced IFN-γ was also observed in *Listeria*-infected (N. M. Tsuji *et al.*, in preparation) and LPS-exposed (G. Ku *et al.*, in preparation) $ICE^{-/-}$ mice.
23. G. Trinchieri, *Annu. Rev. Immunol.* **13**, 251 (1995).
24. F. Belardelli, *APMIS* **103**, 161 (1995); C. A. Dinarello, *Blood* **87**, 2095 (1996).
25. N. Margolis and C. Dinarello, unpublished data.
26. G. Ku and M. W. Harding, unpublished data.
27. D. K. Dalton *et al.*, *Science* **259**, 1739 (1993); S. Huang *et al.*, *ibid.*, p. 1742; B. D. Car *et al.*, *J. Exp. Med.* **179**, 1437 (1994).
28. Y. Takebe *et al.*, *Mol. Cell. Biol.* **8**, 466 (1988).
29. Y. Gu, C. Sarnecki, R. A. Aldape, D. J. Livingston, M. S.-S. Su, *J. Biol. Chem.* **270**, 18715 (1995).
30. H. Quill and R. H. Schwartz, *J. Immunol.* **138**, 3704 (1987).
31. H. Tsutsui, Y. Mizoguchi, S. Morisawa, *Hepato-Gastroenterology* **39**, 553 (1992).
32. We thank T. Fox and W. Chen for ICE and TX protein; A. Diu, C. Faucheu, and J.-L. Lalanne for TX cDNA; M. Rincon for A. E7 cells; J. Lippke for CPP32 and CMH-1 cDNA; B. O'Hare for oligonucleotide synthesis and DNA sequencing; T. Faust for ELISA; A. Heiser for animal surgery; and J. Boger for critical reading and discussion of the manuscript. R.A.F. is an HHMI Investigator.

16 September 1996; accepted 19 November 1996

A Synaptically Controlled, Associative Signal for Hebbian Plasticity in Hippocampal Neurons

Jeffrey C. Magee and Daniel Johnston

The role of back-propagating dendritic action potentials in the induction of long-term potentiation (LTP) was investigated in CA1 neurons by means of dendritic patch recordings and simultaneous calcium imaging. Pairing of subthreshold excitatory postsynaptic potentials (EPSPs) with back-propagating action potentials resulted in an amplification of dendritic action potentials and evoked calcium influx near the site of synaptic input. This pairing also induced a robust LTP, which was reduced when EPSPs were paired with non–back-propagating action potentials or when stimuli were unpaired. Action potentials thus provide a synaptically controlled, associative signal to the dendrites for Hebbian modifications of synaptic strength.

Recent evidence for the presence of voltage-gated Na^+, Ca^{2+}, and K^+ channels in dendrites and the active propagation of action potentials from the axon into the dendrites has required a reevaluation of the mechanisms of synaptic integration and synaptic plasticity in central neurons (*1*). In hippocampal neurons, LTP is thought to occur in response to the simultaneous activation of both pre- and postsynaptic elements (*2*, *3*). Most LTP induction protocols, however, involve prolonged depolarizations of the postsynaptic neuron (*4*). Thus, it is not clear whether under more physiological conditions postsynaptic action potentials are important for LTP induction, as originally suggested by Hebb (*5*). In Hebbian learning theories, correlated synaptic input and action potential output are associated with increases in synaptic strength (*6*). The relatively large physical distance separating the input (dendrites) from the output (axon) creates the need for a rapid feedback signal capable of forming an association between the synaptic input and the action potential output of the neuron. The back-propagating dendritic action potential appears to be ideally suited for such an associative signal. Axonally initiated action potentials (*7*) propagate rapidly into the soma and dendrites, providing large membrane depolarizations and substantial increases in dendritic intracellular calcium ion concentration ($[Ca^{2+}]_i$) (*8*, *9*).

Back-propagating action potentials decline in amplitude with distance from the cell body (*8*, *10*) and fail to propagate beyond certain distal branch points during repetitive firing (*8*). We found that pairing of axonally initiated action potentials with subthreshold EPSPs increased dendritic action potential amplitude and Ca^{2+} influx (Fig. 1) (*11*, *12*). A subthreshold EPSP train produced a small and highly localized increase in $[Ca^{2+}]_i$ (2% $\Delta F/F$ in the region labeled with an asterisk), whereas the unpaired action potential train induced a more widespread, but still relatively small, increase in $[Ca^{2+}]_i$ (5% $\Delta F/F$) (Fig. 1A). Pairing of synaptic stimulation and back-propagating action potentials, however, resulted in an increase in $[Ca^{2+}]_i$ that was significantly larger than the simple sum of the two independent Ca^{2+} signals (10% $\Delta F/F$) (Fig. 1A). The amount of the pairing-induced increase in action potential amplitude and Ca^{2+} influx increased progressively with distance from the cell body (Fig. 2, C and D). When EPSPs and action potentials occurred simultaneously, no significant changes in signal amplitudes were observed in somatic and proximal dendritic regions, whereas large, supralinear increases

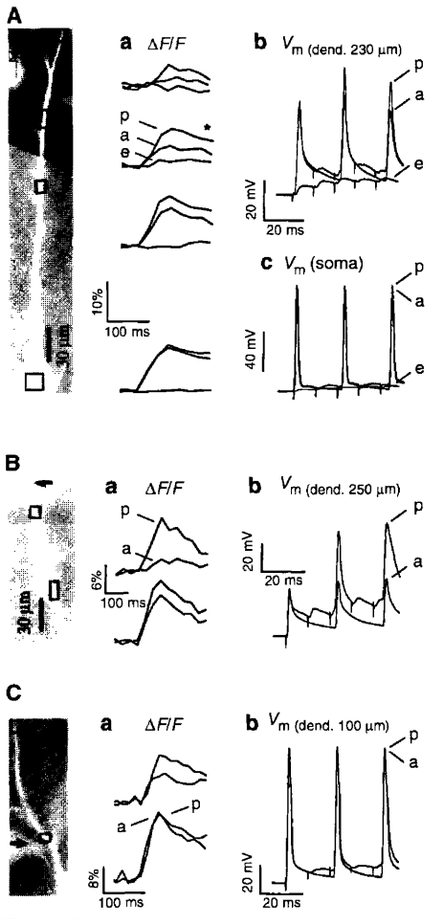

Fig. 1. Dendritic action potential amplitude and evoked Ca^{2+} influx are enhanced by simultaneous synaptic input. (**A**) (Aa) Optical recordings showing average $\Delta F/F$ from regions of the neuron delimited by the boxes shown at left. Traces are from progressively more proximal regions moving down the column in (b). Traces labeled e were recorded during subthreshold EPSPs; a, during unpaired action potentials; and p, during paired action potentials and EPSPs. Synaptic stimulation induced a significant increase in $[Ca^{2+}]_i$ in only the middle set of traces (*).The supralinear increase in $[Ca^{2+}]_i$ during paired EPSPs and action potentials is apparent in the more distal regions of the neuron. There was no such increase in the soma. (Ab) Electrical recordings from the dendrite showing supralinear summation of dendritic action potentials and EPSPs during paired stimulation. Traces are labeled as in (a). (Ac) Electrical recordings from the soma showing paired synaptic activity and action potential generation do not result in an increased action potential amplitude. Traces are labeled as in (b). (**B**) Dual electrical recordings from a neuron showing extreme supralinear summation in both the optical (Ba) and electrical (Bb) dendritic recordings. Unpaired dendritic action potentials appear to be nonregenerative. (**C**) Dual electrical recordings from a more proximal dendritic region. Pairing had little effect on Ca^{2+} entry in lower box (Ca) or on action potential amplitude (Cb). In the more distal optical recording (upper box, 200 μm), a larger increase in $[Ca^{2+}]_i$ during paired stimuli was observed. The locations of dendritic recording pipettes are labeled by arrows.

Division of Neuroscience, Baylor College of Medicine, One Baylor Plaza, Houston, TX 77030, USA. E-mail: jmagee@ptp.bcm.tmc.edu